IEEE Access
Multidisciplinary | Rapid Review | Open Access Journal

Received 23 May 2024, accepted 3 June 2024, date of publication 14 June 2024, date of current version 2 July 2024.

Digital Object Identifier 10.1109/ACCESS.2024.3414450

RESEARCH ARTICLE

A Quadratic Formulation of ESS Degradation and Optimal DC Microgrid Operation Strategy Using Quadratic Programming

KYONG JIN CHOI[1], JAEMIN PARK[2], TAEHYEON KWON[3], (Member, IEEE), SOONHYUNG KWON[4], DO-HOON KWON[4], (Member, IEEE), YOUNG-IL LEE[4], (Senior Member, IEEE), AND MIN KYU SIM[5], (Member, IEEE)

[1]Energy and Environment Research Institute, Seoul National University of Science and Technology, Seoul 01811, South Korea
[2]Department of Data Science, Seoul National University of Science and Technology, Seoul 01811, South Korea
[3]Harold and Inge Marcus Department of Industrial and Manufacturing Engineering, The Pennsylvania State University, University Park, PA 16802, USA
[4]Department of Electrical and Information Engineering, Seoul National University of Science and Technology, Seoul 01811, South Korea
[5]Department of Industrial Engineering, Seoul National University of Science and Technology, Seoul 01811, South Korea

Corresponding author: Min Kyu Sim (mksim@seoultech.ac.kr)

This work was supported by the Basic Science Research Program through the National Research Foundation of Korea (NRF) funded by the Ministry of Education under Grant NRF-2021R1A6A1A03039981 and Grant NRF-2019R1A6A1A03032119.

ABSTRACT Microgrids are fundamental elements in modern energy systems. Among the various microgrid components, the Energy Storage System (ESS) plays a pivotal role in ensuring system reliability, but its high cost and inevitable degradation over time pose significant challenges. Many current studies overlook the impact of ESS degradation on operational optimization, potentially leading to cost-ineffective systems. To address this gap, we introduce a quadratic ESS degradation model that captures intricate battery dynamics, such as State of Charge (SoC) and Depth of Discharge (DoD), using Markovian properties. Based on this model, we propose an optimal energy management framework for DC microgrids using Quadratic Programming (QP). The objective is to minimize the combined costs of degradation and electricity, considering the Time-of-Use (ToU) tariff while adhering to ESS constraints. This financially focused approach provides a pragmatic and economically aligned optimization strategy. Testing across various State of Health (SoH) scenarios demonstrates that our proposed model reduces total operational costs by 3-18%. This research advances microgrid optimization techniques and offers practical insights to enhance efficiency and economic resilience in real-world scenarios.

INDEX TERMS Energy storage system, microgrid, battery degradation, electricity cost, quadratic programming.

NOMENCLATURE

C_t^{GRID}	Unit electricity cost from the grid between time t and $t+1$.
P_t^{GRID}	Power flow from the AC to the microgrid between time t and $t+1$.
P_t^{ESS}	Power inflow into the ESS between time t and $t+1$.
P_t^{PV}	Power generated by solar power system between time t and $t+1$.
P_t^{LOAD}	Power consumption of the microgrid system between time t and $t+1$.
B_t^{SoC}	SoC of an ESS at time t.
$\mathbf{C}^{GRID}$	Vector of C_t^{GRID} values from time 0 to T.
$\mathbf{P}^{GRID}$	Vector of P_t^{GRID} values from time 0 to T.
$\mathbf{P}^{ESS}$	Vector of P_t^{ESS} values from time 0 to T.
$\mathbf{P}^{PV}$	Vector of P_t^{PV} values from time 0 to T.
$\mathbf{P}^{LOAD}$	Vector of P_t^{LOAD} values from time 0 to T.
$\mathbf{B}^{SoC}$	Vector of B_t^{SoC} values from time 0 to T.

The associate editor coordinating the review of this manuscript and approving it for publication was Wencong Su.

c_{new}	Cost of a new ESS unit.
$\bar{L}_t$	SoH of an ESS at time t.
q^{ESS}	Energy capacity of the ESS (kWh).
$S_\delta(\delta)$	DoD stress factor.
$S_\sigma(\sigma)$	SoC stress factor.
$S_T(T)$	Temperature stress factor.
$S_t(t)$	Time stress factor.
α_{sei}, β_{sei}	Coefficients for SEI film formation in the battery degradation model.
$f_{d,1}$	Degradation per cycle.
β_0, β_1, β_2	Coefficients of the battery degradation approximation model.
$\mathbb{1}_N$	N-dimensional vector with each element having a value of 1.
I_N	N×N identity matrix.
$\mathbf{M}$	N×N matrix with $\mathbf{M}_{ij} = \begin{cases} 1, & \text{if } i > j \\ 0, & \text{otherwise.} \end{cases}$
$\mathbf{M}'$	N×N matrix with $\mathbf{M}'_{ij} = \begin{cases} 1, & \text{if } i \geq j \\ 0, & \text{otherwise.} \end{cases}$

I. INTRODUCTION

Microgrids, typically equipped with a photovoltaic (PV) system and an energy storage system (ESS), play an essential role in the modern power system landscape by offering enhanced resilience, sustainability, and energy efficiency [1], [2].

ESS stands out as a pivotal component in microgrids, providing economic benefits by storing volatile renewable energy sources such as PV and wind. It also enables the effective redistribution of energy from off-peak to peak hours. However, ESS does not function perpetually; its economic benefits are constrained by inherent degradation properties.

Batteries, as the predominant form of ESS, undergo degradation, marked by a progressive decline in capacity over time and repeated charge-discharge cycles. From an economic perspective, this degradation should be viewed as depreciation. Accurately accounting for battery degradation is crucial for efficient microgrid operation.

Considering the non-linear and complex nature of battery degradation, however, many studies on microgrid optimization fail to adequately address this issue, as indicated by the omission in [3] and the simplified approaches in [4], [5], [6], [7], [8], [9], and [10]. The limitations in addressing battery degradation primarily appear in two forms:

1) Oversimplification of degradation models: Numerous models fall short of capturing the complete range of battery usage patterns by neglecting crucial factors such as State of Charge (SoC) and Depth of Discharge (DoD), which are the primary drivers of degradation [11]. To illustrate, while the studies [6], [7] exclusively emphasized DoD, they did not consider the significance of SoC. Conversely, the study of [8] primarily considered on SoC in their degradation model. The authors of [9] simplified the battery degradation model by linearizing it into two distinct segments. In a different case, despite [10] aiming to incorporate a comprehensive degradation model from [11], the study made a simplified assumption that battery capacity linearly declines with cycle increments, thus overlooking the evident nonlinear decay observed in a battery's early life, as suggested by [11].
2) Limited consideration of monetary aspects: The costs associated with degradation are rarely expressed in monetary terms. For instance, in the study [4] penalties are applied to battery charging and discharging activities to minimize battery operations within specified limits. The authors of [5] included battery power in the cost function to prolong battery life. However, these penalties are not converted into financial values.

To resolve the two aforementioned battery degradation issues, an accurate battery degradation model is paramount before devising an optimal ESS operation strategy. Various endeavors have been undertaken to formulate accurate battery degradation models [11], [12], [13], [14], [15], [16]. The seminal degradation model proposed by [11] has successfully captured the non-linearity of degradation by considering both the SoC and DoD. The authors of [11] empirically demonstrated the model's robust correlation with real-world scenarios. However, the need for historical data in its Rainflow counting method inherently limits its applicability in real-time decision-making. To overcome the necessity of historical data, the study [16] reformulated the model of [11] into a Markovian model to ensure that the current state of the battery contains sufficient information on future battery degradation.

To illustrate the use of the Markovian degradation model, the study [16] framed the ESS operation problem as a Markovian Decision Process (MDP) and tackled it using a learning-based algorithm, Reinforcement Learning (RL). However, the Markovian degradation model proposed by [16] includes a numerical procedure for solving nonlinear equations, which presents compatibility issues with general mathematical optimization methods such as Linear Programming (LP) and Quadratic Programming (QP).

Our degradation model aims to refine the existing models to be fit for analytical optimization methods. While authors of [16] presented a Markovian model reformulated from the model by [11], their model needed iterations for approximation. Building upon the seminal contributions of [11] and [16], our quadratic degradation model further simplifies and transforms it into a mathematical form suitable for analytical optimization methods. Furthermore, by providing an analytical equation, our model can reduce the computational burden of calculations and enhance interpretability. We have

analytically refined their frameworks, ensuring our model accurately accounts for the degradation cost in the monetary term. To summarize, our degradation model comprises three crucial attributes: increase efficiency and interpretability, fidelity to foundational works, monetary evaluation, and adaptability to mathematical optimization frameworks. These elements collectively render it an indispensable tool for effectively optimizing microgrid systems.

This study pursues the optimization of microgrid operation using QP that incorporates the proposed quadratic degradation model. While RL is a robust technique capable of operating in ill-defined environments [17], it presents several challenges. First, RL does not ensure a global optimum solution. Its reliance on a trial-and-error approach, which is heavily influenced by initial conditions and the agent's particular experiences, can lead to suboptimal outcomes. Second, RL often encounters difficulties in handling explicit constraints, potentially yielding solutions that might be infeasible or unsafe for microgrid operations. Finally, alterations in system parameters require retraining, which is an inefficient process for microgrids that undergo frequent changes.

In our research, we adopt the QP approach that overcomes the aforementioned limitations of RL. QP excels in contexts where systems have robust predictive models [18]. As prediction models for PV generation and power demand continue to improve, they form a dependable foundation for microgrid optimization [19], [20], [21]. QP not only handles practical constraints intrinsic to control problems, such as stability requirements and input-output boundaries but also ensures the feasibility and safety of microgrid operations [22]. Additionally, the deterministic nature of QP allows for efficient adaptations in response to the changes in system parameters, establishing it as a resilient tool in dynamic microgrid settings [23].

In microgrid optimization research, several studies strongly advocate for multiobjective optimization [23], [24], [25], [26], [27], [28], [29]. These studies incorporate a wide range of considerations, covering primary operational costs to ancillary factors such as battery degradation, emission of pollutant gases, strategic node selection, and the stability of power generation.

In particular, the study [23] demonstrates the effectiveness of QP in optimizing the energy management of microgrids. The authors propose an objective function that integrates two distinct components: electricity costs and battery degradation. However, these components are measured in different units, with electricity costs quantified in monetary terms and battery degradation gauged in units related to battery life or performance decline. The integration of these heterogeneous units requires careful consideration. The weighted addition of heterogeneous terms can be arbitrary, lacking a clear rationale or systematic determination method. This limitation calls for expressing the lifespan and degradation of the battery in monetary terms.

Studies [24], [25] focus on reducing CO_2 emissions, while [26] expands its objectives to include the emission of multiple pollutants and cost considerations. Studies [27] and [28] address power variability in microgrid systems, with [27] emphasizing effective node connections and [28] integrating environmental costs. The authors of [29] implemented four different objectives, including costs, into their optimization problem.

In contrast to the earlier examinations of multiobjective optimization, our study presents multiple objectives consistently quantified in monetary units. This requires a detailed understanding of the diverse cost elements inherent in microgrid operations, including battery degradation and Time-of-Use (ToU) tariffs. By integrating a quadratic ESS degradation model, we refine the conventional QP formulation, forging a framework that prioritizes pragmatic monetary optimization.

This paper contributes in the following aspects:

- proposing a quadratic battery degradation model that reduces computational burden compared to existing models while preserving a high level of accuracy and encompasses both the SoC and DoD.
- formulating the microgrid optimization with explicit monetary evaluation, ensuring battery degradation costs are adequately considered,
- employing QP for microgrid optimization, factoring in battery degradation, which results in a substantial operational cost reduction of 3-18 %.
- proposing QP-based optimization model exploits the convexity, ensuring global optimality while reducing computational complexity. This enables real-time decision-making and integration into microgrid management.

II. DEGRADATION MODEL

In recent years, the development of battery degradation models has been actively researched, yet a consensus on a definitive model has not been reached. This section introduces a noteworthy approach to characterizing battery degradation. Given its complexity and the challenges it poses for direct application in diverse scenarios, such as operational management of ESS, a simplified quadratic approximation of the original model is proposed. The validation of this approximation model is then examined.

A. PREVIOUS RESEARCH ON BATTERY DEGRADATION

Given that the extent of battery degradation is affected by usage patterns and external factors, comprehending the properties of degradation is essential, particularly considering the high cost of the battery [30]. This section delves into the semi-empirical battery degradation model from [11] and its numerical reformulated version with Markovian property by [16], underscoring their relevance in optimizing microgrid systems.

Battery degradation, a nonlinear process, can be categorized into cycle aging and calendar aging [14], [15].

Cycle aging results from repeated charging-discharging activities, while calendar aging refers to the battery's natural wear over time, influenced by factors such as SoC and environmental temperature. The study [14] presents a chemical model of factors contributing to battery degradation. Building upon this, the foundational research by [11] outlines the stress factors leading to degradation and proposes a mathematical framework. The study [11] links two aging types to four stress factors:

- SoC stress, $S_\sigma(\sigma)$: Degradation increases with higher SoC levels; maintaining lower SoC levels helps mitigate degradation.
- DoD stress, $S_\delta(\delta)$: Degradation increases super-linearly with DoD levels, accelerating at a rate greater than proportional to increases in DoD.
- Temperature stress, $S_T(T)$: Degradation varies with the operating temperature. Temperatures between 15°C and 20°C are optimal for minimizing degradation.
- Time stress, $S_t(t)$: Batteries degrade over time, independent of cycling.

Temperature and time stresses, which contribute to battery degradation, are presumed to be minimized in the controlled microgrid environment, where conditions are carefully managed to avoid extreme temperatures. While acknowledging the impact of numerous factors on battery degradation that are not included in our model, our study focuses on controllable factors, consistent with the approach taken by [11].

The degradation per cycle, $f_{d,1}$, is calculated by combining these factors as shown in Equation (1) below.

$$f_{d,1} = (S_\delta(\delta) + S_t(t)) \times S_\sigma(\sigma) \times S_T(T) \tag{1}$$

$f_{d,1}$ effectively estimates the battery lifespan in a fixed charge-discharge cycle, enabling the computation of the battery life $\bar{L}_t$.

$$\bar{L}_t = 1 - \alpha_{sei} e^{-N_t \beta_{sei} f_{d,1}} - (1 - \alpha_{sei}) e^{-N_t f_{d,1}} \tag{2}$$

where α_{sei} and β_{sei} represent coefficients for solid electrolyte interphase (SEI) film formation in the battery degradation model, and N_t represents the number of cycles.

Although Equation (2) offers a method to compute battery degradation within a fixed charge-discharge cycle, it is not fully suited for real-world scenarios that exhibit irregular battery usage patterns. To tackle this limitation, the study [11] employed the Rainflow counting method [31]. However, this approach requires an exhaustive battery operation history which poses computational challenges during optimization [16]. To address this challenge, the authors of [16] present a Markovian reformulation for the battery degradation model. Markovian models are state-dependent, thereby avoiding the need for extensive historical data, which greatly improves computational efficiency.

For the determination of battery life, the Markovian approach uses three key metrics: the current SoH ($\bar{L}_t$), current SoC (B_t^{SoC}), and next SoC (B_{t+1}^{SoC}). These values facilitate the prediction of the SoH for the next time step ($\bar{L}_{t+1}$).

$$\bar{L}_{t+1} = f(\bar{L}_t, B_t^{SoC}, B_{t+1}^{SoC}) \tag{3}$$

Equation (3) takes a Markovian form, predicting the SoH at the next time step based on the current and next time step's SoC and the current SoH, assuming constant values for other environmental variables. This method is crucial for determining optimal charging and discharging times. It forecasts the battery's lifespan through variations in the SoC, reflecting the user's battery usage patterns. The study [16] proposed a numerical procedure for Equation (3) and demonstrated it to be a highly loyal model with an error of less than 0.001% compared to the original model in [11]. To further refine this model, we propose its quadratic approximation form in the next subsection.

B. QUADRATIC APPROXIMATION OF THE BATTERY DEGRADATION MODEL

The Markovian degradation model proposed by [16] improved computational efficiency and showed compatibility with RL frameworks compared to the model by [11]. However, the iterative process in numerical methods makes it challenging to use analytical optimization methods like QP. To address this, we introduce a quadratic approximation of the battery degradation model, enabling its integration with analytical optimization methods. The specific revisions are as follows.

Figure 1 illustrates SoH changes for three fixed SoC cycles. For instance, "Cycle 85-25" shows the SoH impact of repeatedly operating the battery between 85% and 25% SoC. Figure 1 reveals a progressive shift from nonlinear to relatively linear SoH changes as the number of battery cycles increases.

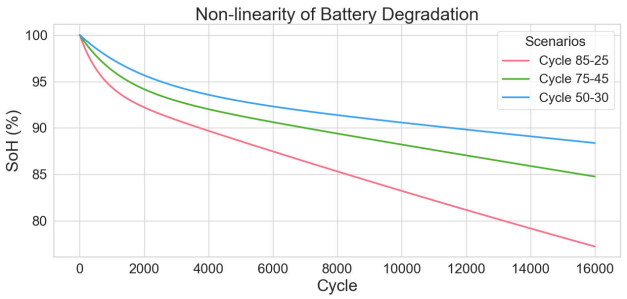

FIGURE 1. Non-linearity of battery degradation.

Due to pronounced nonlinearity in certain intervals, we employ piecewise regression. Considering batteries are often disposed of when their SoH reaches around 80%, our model focuses on the SoH range from 100% to 80%. The following steps are taken to develop our degradation model: 1) Employing piecewise division for SoH intervals, 2) Generating training data, 3) Training the model, and 4) Validating the model.

To effectively address the nonlinearity of degradation, we applied a piecewise regression approach, segmenting the

SoH into distinct intervals and creating a regression model for each. For the SoH range of 100%-90%, which exhibits pronounced nonlinearity, we developed models for each 1% segment. Given that the SoH range of 90%-80% shows comparatively linear degradation, we utilized a single, unified model to represent this interval. In total, 11 models were developed to characterize the battery degradation for the SoH range of 100% to 80%.

Furthermore, the generation of robust training data is vital for the development and validation of our models. We generated a training dataset by simulating different scenarios using the Markovian degradation model proposed by [16]. Specifically, we generated the training dataset as follows. First, 10,000 pairs of uniform random SoC and the next SoC were generated. For each pair, the DoD was calculated to form an input sample consisting of SoC, the next SoC, and DoD values. Second, for each input, the SoH degradation was calculated using the Markovian degradation model to determine the output value. Finally, regression was used on this training data to obtain a quadratic model. Our dataset, which incorporates a range of degradation outputs from the model, ensures an accurate representation of complex degradation properties.

In the process of training the model using data generated with hourly ESS control intervals, we assumed that external stress factors, such as time and temperature stresses, exhibit minimal variations across cycles. As a result, the SoH is determined solely by the SoC ($(B_t^{SoC} + B_{t+1}^{SoC})/2$) and DoD ($|B_t^{SoC} - B_{t+1}^{SoC}|$). Using our proposed regression method, we derived the following model for per-cycle SoH variation:

$$\bar{L}_t - \bar{L}_{t+1} = \beta_0 + \beta_1 \frac{B_{t+1}^{SoC} + B_t^{SoC}}{2} + \beta_2 |B_{t+1}^{SoC} - B_t^{SoC}|^2 + \epsilon_t. \quad (4)$$

Here, ϵ_t denotes the residual term, capturing any unexplained variability.

To assess the performance of our trained models, we employed the R^2 metrics. Figure 2 provides a comparison of values between the Markovian and the quadratic model across 300 random samples for both the 80%-90% and 96%-97% SoH intervals. A perfect alignment between models would position all data points along the red dashed 45-degree diagonal line. For SoH values in the 80%-90% range, the model achieved an R^2 of 0.98. In the nonlinear 90%-100% SoH region, where piecewise regression was applied, all 10 models consistently achieved scores above 0.97, including the 96%-97% SoH interval. Incorporating higher-dimensional SoC and DoD variables did not lead to a significant improvement in fit.

Our quadratic model closely approximates the Markovian degradation model proposed in the study by [16], demonstrating a strong goodness of fit. Unlike the models presented in the studies by [11] and [16], our proposed model directly provides degradation equations for variable SoC usage patterns, enabling the formulation of optimization problems for analytical methods.

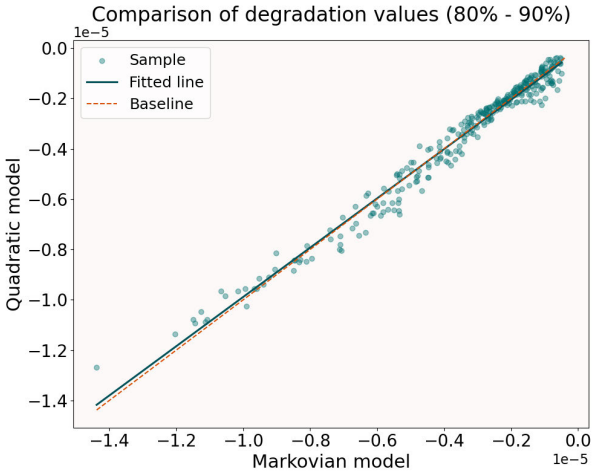

(a) SoH 80% - 90%

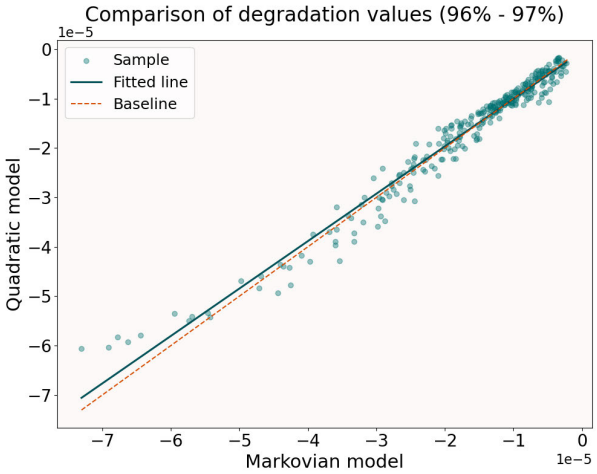

(b) SoH 96% - 97%

FIGURE 2. **Comparison of degradation values.**

III. QP PROBLEM DESCRIPTION

In this section, we explore the application of our previously introduced quadratic degradation model to a concrete microgrid scenario, presenting a detailed problem formulation reminiscent of the challenges addressed in [23]. Our setup, as depicted in Figure 3, demonstrates the system architecture central to our QP optimization approach tailored for microgrids.

Our analysis is centered around a university campus equipped with PV and ESS. In our configuration, the PV system feeds into a DC-bus, transferring its generated power, P^{PV}, to the grid. A controller governs whether the ESS charges or discharges from the DC-bus, with a positive P^{ESS} signaling charging and a negative indicating discharging. An Active Front End (AFE) AC/DC converter links the DC bus to an AC power supplier, with the purchased power labeled P^{GRID}. Due to the ToU tariff structure, the purchase cost is dynamic. The microgrid system can then draw its required electricity, P^{LOAD}, from diverse sources.

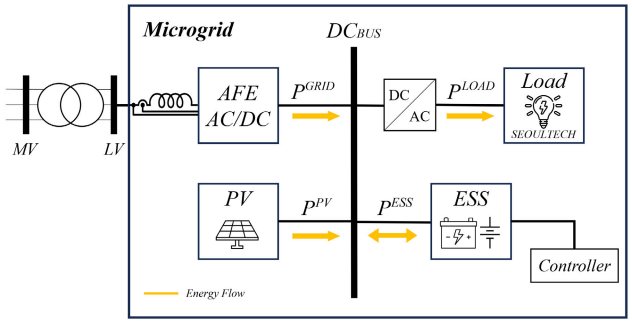

FIGURE 3. DC microgrid architecture.

In line with the objectives outlined in [23], our primary goal is to minimize the microgrid's operating costs, with a specific focus on optimizing ESS control within system constraints using QP. We believe that highlighting the advantages of our QP optimization compared to the Markovian degradation model [16] for ESS management in microgrids aids in understanding the detailed description of the mathematical unfoldings in this section:

- Efficiency: Our method outperforms in scenarios with well-defined parameters, aligning with ESS management needs while optimizing computational resources.
- Simplicity: By using the piecewise quadratic regression, our method facilitates straightforward implementation due to its analytical nature and compatibility with the system model.
- Determinism: This approach ensures consistent outcomes when the input is identical, which is crucial for stable microgrid operations.

A. OBJECTIVE FUNCTION

The primary expenses associated with operating a microgrid system are electricity costs and ESS depreciation costs. To address these, our objective function J aims to minimize these costs over the time interval from 0 to $N-1$, considering a fixed time interval of one hour. With this understanding, we formulate J for optimal ESS operation as follows:

$$J = min \sum_{t=0}^{N-1} \{C_t^{GRID} P_t^{GRID} + c^{new} |\bar{L}_{t+1} - \bar{L}_t|\}. \quad (5)$$

In this function, C_t^{GRID} denotes the electricity tariff at varying times, P_t^{GRID} stands for the power transferred from the AC grid to the microgrid at time t, and c^{new} is the cost of a new ESS system. This formulation rectifies the unit inconsistency observed in the model from [23] and presents a cost function framed strictly in monetary terms.

B. CONSTRAINTS

The input power (P_t^{GRID}), the power of the ESS (P_t^{ESS}), and the SoC level (B_t^{SoC}) have the following boundaries in all segments.

$$P_{min}^{GRID} \le P_t^{GRID} \le P_{max}^{GRID} \quad (6)$$
$$P_{min}^{ESS} \le P_t^{ESS} \le P_{max}^{ESS} \quad (7)$$
$$B_{min}^{SoC} \le B_t^{SoC} \le B_{max}^{SoC} \quad (8)$$

The only controllable variable in the system is the power of the ESS (P_t^{ESS}), which assumes a positive value during charging and a negative value during discharging. As a result, all other variables, such as P_t^{GRID} and B_t^{SoC}, should be expressed in terms of P_t^{ESS}.

In this microgrid system, the input power (P_t^{GRID}) is determined by subtracting the power generated by the solar power system (P_t^{PV}) from the sum of the ESS (P_t^{ESS}) and the microgrid system's power consumption (P_t^{LOAD}).

$$P_t^{GRID} = P_t^{ESS} + P_t^{LOAD} - P_t^{PV} \quad (9)$$

On the other hand, the SoC level (B_t^{SoC}) is determined by the power of the ESS (P^{ESS}) and the ESS capacity (q^{ESS}).

$$B_t^{SoC} = B_{t-1}^{SoC} + \frac{P_{t-1}^{ESS}}{q^{ESS}}. \quad (10)$$

Additionally, from the above equation, we deduce that the SoC is measured relative to a new battery's capacity rather than its degraded state, as the ESS capacity remains fixed at its initial value. This recurrence relation (10) can be expressed as the cumulative value of P^{ESS}.

$$B_t^{SoC} = B_0^{SoC} + \sum_{i=0}^{t-1} P_i^{ESS} / q^{ESS} \quad (11)$$

C. MATRIX REPRESENTATION OF QP

To adapt the existing software to this problem, a transition is implemented to a matrix representation. Using the vector $\mathbf{P}^{ESS}$, where each element corresponds to the P_t^{ESS} value for a segment, we can frame the objective function as follows:

$$J = \min_{\mathbf{P}^{ESS}} \frac{1}{2} (\mathbf{P}^{ESS})^T \mathbf{Q} \mathbf{P}^{ESS} + \mathbf{b} \cdot \mathbf{P}^{ESS}, \quad (12)$$

where

$$\mathbf{Q} = \frac{2c^{new}\beta_2}{(q^{ESS})^2} \mathbf{I_N} \quad (13)$$
$$\mathbf{b} = \mathbf{C}^{GRID} + \frac{c^{new}\beta_1}{q^{ESS}} (\mathbf{M} + \mathbf{M}')^T \mathbb{1}_N \quad (14)$$

A detailed derivation is available in the Appendix.

Here, $\mathbf{I_N}$ represents an N-dimensional identity matrix, and $\mathbb{1}_N$ is an N-dimensional vector with values of 1. $\mathbf{M}$ is an N-dimensional square matrix where all strictly lower triangular elements are 1 and the rest are 0. $\mathbf{M}'$ is a matrix obtained from $\mathbf{M}$ by changing only its diagonal elements to 1.

The input power (P_t^{GRID}) constraint in (6) and the ESS power (P_t^{ESS}) constraint in (7) are related to Equation (9). For an efficient solution-finding method, these constraints can be

combined to define the upper and lower bounds of ESS power (P^{ESS}) as follows.

$$P_i^{LB} = max\{P_{min}^{GRID} - P_i^{LOAD} + P_i^{PV}, P_{min}^{ESS}\}$$
$$P_i^{UB} = min\{P_{max}^{GRID} - P_i^{LOAD} + P_i^{PV}, P_{max}^{ESS}\}$$

By introducing vectorized representation of P_t^{LB}, P_t^{UB} into $\mathbf{P}^{LB}$, $\mathbf{P}^{UB}$, the constraints (6), (7), and (8) are organized in the following matrix form.

$$\begin{pmatrix} \mathbf{I}_N \\ -\mathbf{I}_N \\ \mathbf{M} \\ -\mathbf{M} \end{pmatrix} P_{ESS} \leq \begin{pmatrix} \mathbf{P}^{UB} \\ -\mathbf{P}^{LB} \\ q^{ESS}(B_{max}^{SoC} - B_0^{SoC})\mathbb{1}_N \\ q^{ESS}(-B_{min}^{SoC} + B_0^{SoC})\mathbb{1}_N \end{pmatrix}$$

IV. RESULTS AND DISCUSSION

This section designs and performs an empirical study of the proposed problem. Throughout this simulation study, we aim to address the following three questions.

1) Does the adaptation of the proposed quadratic degradation model into ESS operation lead to cost savings?
2) How does the consideration of degradation property impact the usage pattern of the ESS?
3) How does the usage pattern of the ESS vary across the lifespan of the ESS?

A. THE DATA-DRIVEN SIMULATION DESCRIPTION

The dataset used in our study is derived from the operation of the microgrid system at Seoul National University of Science and Technology (Seoul-Tech), located in Seoul, South Korea, in July 2022. The electricity consumption of the microgrid system for the month was 1,876 kWh, accounting for approximately 3-4% of SeoulTech's total electricity consumption. The PV system accounts for about 13% of the microgrid's total power consumption, with the remaining portion to be purchased from the external grid. The simulations described in this study were conducted using Python with the CVXOPT library version 1.3.2, chosen for its robust capabilities in handling complex optimization problems.

Table 1 summarizes the constants related to the optimization problem discussed in the previous section. The external power input into the microgrid is expressed as a positive value, limited to a maximum of 200 kW to prevent exceeding the system's peak load. This restriction ensures the prevention of power shortages and any potential impact on the operation of the ESS. The ESS functions within a -50 kW to 50 kW range, with negative values denoting discharge and positive indicating charge. To mitigate risks of overcharging and deep discharging, the SoC of the ESS is restricted to a range between 20% and 80%, with an initial SoC set at 50%. This operational constraint is informed by studies [32], [33], [34] which note that such SoC limitations can enhance battery safety, longevity, and reduce its internal resistance.

The ESS comprises three batteries, each with a capacity of 183 kWh, totaling 549 kWh. The cost of a new battery

TABLE 1. Parameter values.

Parameter	Value	Note
$(P_{Min}^{GRID}, P_{Max}^{GRID})$	(0 kW, 200 kW)	
$(P_{Min}^{ESS}, P_{Max}^{ESS})$	(-50 kW, 50 kW)	Negative indicates discharging
$(B_{Min}^{SoC}, B_{Max}^{SoC})$	(20%, 80%)	
B_0^{SoC}	50%	Initial SoC level
q^{ESS}	549 kWh	ESS capacity
c^{new}	1,070,550,000 KRW	Multiplied the original price of the ESS by 2.5, assuming that the ESS is discarded when its SoH drops to 80%, and the residual value of 50% of its value when new
C^{GRID}	52.6 KRW/kWh 97.3 KRW/kWh 163.2 KRW/kWh	Off-peak hours:0-9, 23-24 Mid-peak hours: 9-10, 12-13, 17-23 On-peak hours: 10-12, 13-17

is 428,220,000 KRW, equivalent to approximately $317,220, based on an exchange rate of 1,350 KRW/$. Assuming the residual value of the battery at end-of-life to be zero and the battery to be unusable when its SoH declines from 100% to 80%, the depreciation expense for each 1% reduction in SoH is 5% of the cost of a new battery. Therefore, c^{new} in Equation (5) should be five times the cost of a new battery. Notably, the actual end-of-life value of a battery is rarely zero, and assessing this value is complex. For our analysis, we take a conservative stance on battery degradation and set the residual value at 50% of the cost of a new battery. While this assumption may seem arbitrary, our results show that adjusting the residual value influences numerical outcomes without altering the main conclusion of our study. This adjustment sets c^{new} at 2.5 times the cost of a new battery, equating to 1,070,550,000 KRW.

Concerning the battery disposal occurring at an SoH of 80% and the limitation of ESS operation to an SoC below 80%, the following points need to be addressed. As previously indicated in Equation (10), SoC is gauged against the capacity of a new battery. Despite the battery's degradation and diminished charging capacity, the maximum charging threshold is maintained at 80% of a new battery's capacity, aligning with the operational constraints of the ESS until disposal.

The ToU pricing for the microgrid system is depicted in Figure 4. Rates are tiered into three levels: on-peak hours are marked by red stripes at 163.2 KRW/kWh; mid-peak hours by yellow stripes at 97.3 KRW/kWh; and off-peak hours in white at 52.5 KRW/kWh. Higher rates correspond to periods of elevated electricity demand. A special reduced rate is applied during the lunch hour from 12:00 to 13:00, which is pivotal for the operation of the ESS, a point to be discussed further.

The power readings from the grid, PV, and load, initially captured at 5-second intervals, were averaged to align with our ESS's hourly operational cycle. Consequently, the P^{ESS} vector consists of 744 (24×31) data points. The solution, P^{ESS}, for the optimal operation of the ESS, was derived from

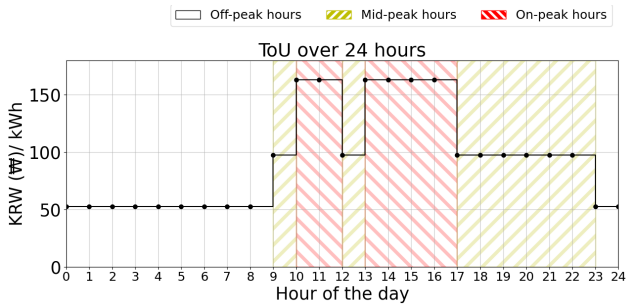

FIGURE 4. ToU over 24 hours.

the objective function defined in Equation (5) under three scenarios: excluding degradation effects (where c^{new} is zero), with moderate sensitivity to degradation at SoH levels from 80% to 90%, and with high sensitivity to degradation from 96% to 97%. Given that daily variations are not significant, average daily results are presented and analyzed. First, the operational costs of the microgrid for each scenario are compared, followed by a detailed examination of how the ESS operation patterns differ across the scenarios.

B. MICROGRID OPERATION COST

This section delves into the first of the three questions outlined earlier. We present the operational costs of the microgrid as defined in Equation (5) and compare them to a scenario where the degradation term is absent, effectively setting c^{new} to zero. This comparison is made to contrast our model with the one presented in a previous study [23], which did not adequately consider the appropriate degradation factors in its ESS optimization model.

Without considering battery degradation, microgrid optimization focuses solely on electricity rates, which may lead to a shorter lifespan of the expensive ESS. The analysis is conducted under two conditions: one where ESS degradation is less significant (an older battery with a SoH between 80%-90%), and another where the degradation is more substantial (a newer battery with SoH between 96%-97%).

Table 2 provides a summarized comparison of the monthly costs associated with the operation of the ESS, both with and without accounting for degradation. The analysis starts by examining a battery with a SoH between 80%-90%. When degradation is not considered, the monthly electricity bill is calculated to be 4,327,000 KRW. Accounting for degradation within the SoH range of 80%-90% causes a marginal increase in the bill to 4,358,000 KRW. However, when degradation is accounted for within the SoH range of 80%-90%, the cost attributable to depreciation is substantially reduced from 1,013,000 KRW to 824,000 KRW. As a result, the total cost excluding degradation effects is approximately 3% higher, totaling 5,340,000 KRW compared to 5,182,000 KRW when degradation is considered.

TABLE 2. Microgrid operation cost (1,000 KRW).

	Electricity	Depreciation	Total
SoH [80%, 90%]			
Model w/o degradation	4,327(81%)	1,013(19%)	5,340(100%)
Model w/ degradation	4,358(84%)	824(16%)	5,182(100%)
Cost saving (diff.)	-31	189	158
SoH [96%, 97%]			
Model w/o degradation	4,327(46%)	5,089(54%)	9,416(100%)
Model w/ degradation	4,996(65%)	2,697(35%)	7,693(100%)
Cost saving (diff.)	-699	2,392	1,723

The impact of degradation is further highlighted within the SoH range of 96%-97%, where the effects per cycle are more severe. When degradation is excluded from the ESS operation, it leads to a monthly depreciation cost of 5,089,000 KRW, which is strikingly over half of the total monthly expenses, overshadowing the regular electricity bill. In contrast, considering degradation raises the electricity bill to 4,996,000 KRW but significantly reduces the depreciation costs to 2,697,000 KRW, culminating in an overall expense of 7,693,000 KRW. This is substantially lower than the 9,416,000 KRW incurred when degradation is disregarded, indicating an 18% rise in costs. In the microgrid domain, where the cost of ESS is significant, our model's consideration of degradation factors plays a crucial role. By accurately capturing the impact of degradation on the overall operational costs, our approach demonstrates its effectiveness in optimizing microgrid performance while minimizing expenses associated with ESS degradation.

C. OPERATIONAL PATTERNS WITH AND WITHOUT DEGRADATION CONSIDERATION

In addressing the second research question, this section evaluates the impact of degradation consideration on the usage patterns of the ESS. A comparative analysis between operational strategies, with and without degradation, is conducted to understand their implications on the battery's SoH.

Figure 5 showcases the average hourly optimal P_t^{ESS} values and the corresponding SoC fluctuations over a month. These are observed under three distinct scenarios: a) where degradation is not included in the model, b) with the battery's SoH ranging from 80%-90%, and c) at a SoH of 96%-97%. The plotted points represent the average P_t^{ESS} for each hour, taken across a month-long period.

From Figure 5 (a), we note that the battery's charging cycle commences at 23:00 to coincide with the lowest electricity rates and continues until the SoC attains the 80% threshold. Afterward, the battery discharges during peak pricing periods. The regression equation (4) highlights a direct correlation between SoC and degradation, indicating that high SoC levels are not cost-effective once degradation is factored into the costs. In response, Figure 5 (b) illustrates how the charging onset is deliberately delayed when degradation is considered, with the SoC only reaching 80% by 9:00, thereby aligning with the beginning of mid-peak hours.

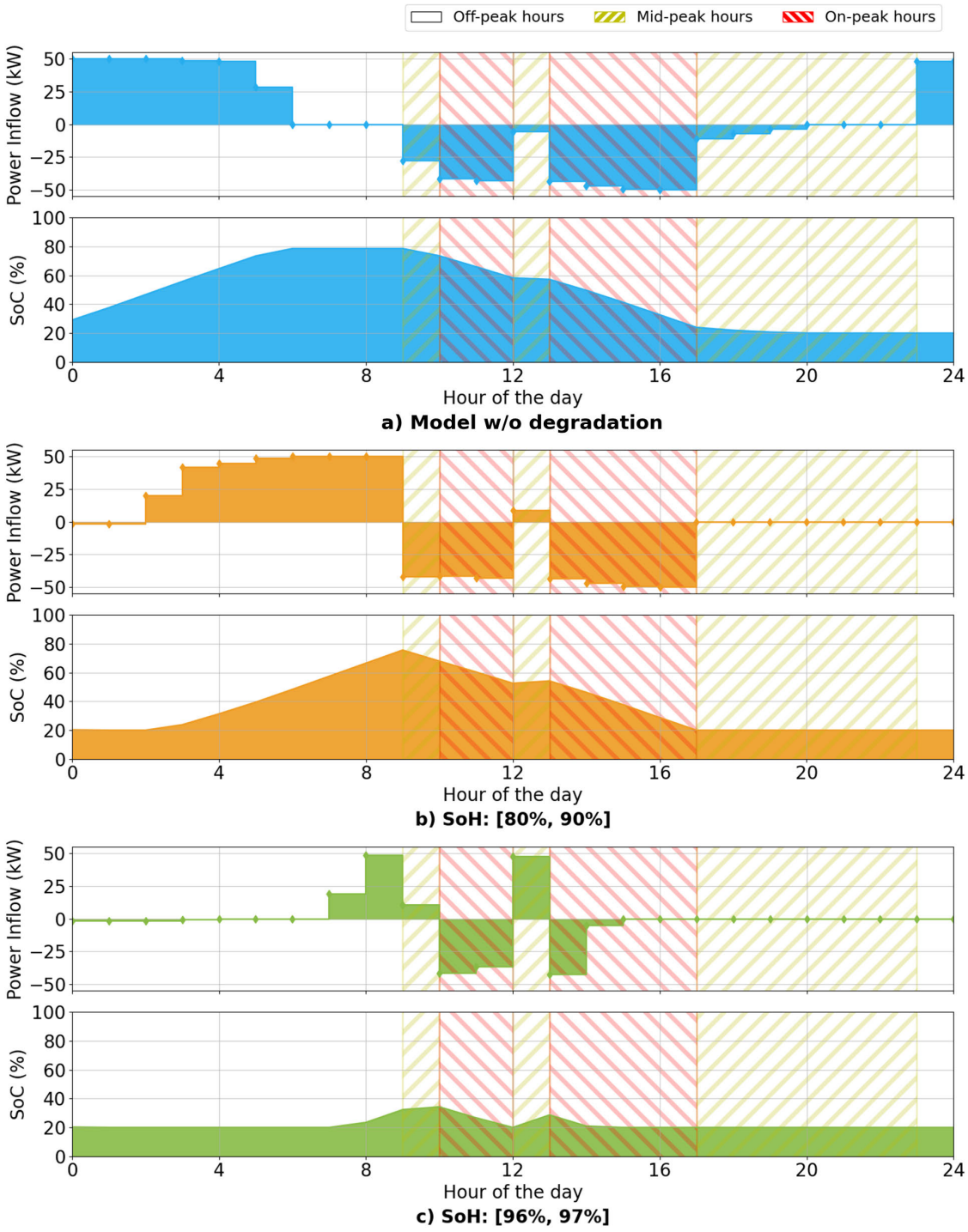

FIGURE 5. Daily averaged optimal ESS power inflow (P^{ESS}) and SoC (B^{SoC}).

Furthermore, a comparison of SoC levels between Figure 5 (a) and (b) reveals that while the SoC peaks at 80% by 6:00 in (a), it does so at 9:00 in (b), indicating a strategic shift in charging times to accommodate degradation effects.

Additionally, a closer examination of the 9:00 to 10:00 interval across both figures reveals a discrepancy: Figure 5 (b) registers a significant discharge, which is then offset by a charging period from 12:00 to 13:00. As the electricity rates remain constant during these intervals, the observed

discharge and subsequent charge cannot be justified by rate differences alone. Instead, this pattern emerges from the need to mitigate degradation, which is more costly at higher SoC levels. Therefore, despite the immediate costs associated with charging, the inclusion of degradation into the operational strategy proves to be more advantageous when assessing the cumulative impact on the efficiency and cost of the system.

D. IMPACT OF SEVERE DEGRADATION ON ESS USAGE PATTERNS

This section tackles the last research question proposed earlier: With increased sensitivity to battery cycles, what variations can be observed in the operational patterns of the ESS?

The operation of a nearly new battery, which suffers more significant degradation with each charging cycle, is depicted in Figure 5 (c). This figure demonstrates a cautious operational approach within the microgrid, maintaining the SoC below 40%. This conservative charging behavior is pronounced, with the battery opting to charge primarily between 9:00 and 10:00, the mid-peak hours. In comparison to Figure 5 (b), the charging activity between 12:00 and 13:00 is substantially higher. These operational decisions are strategic, deliberately aiming to minimize SoC levels to mitigate the high costs associated with battery degradation. Despite opportunities to charge more economically, the priority is to consistently maintain a low SoC, which is beneficial in curtailing degradation linked to DoD fluctuations.

This strict restriction on ESS activity may imply that, given the current conditions, the costs linked with the ESS may surpass the advantages of fully leveraging ToU tariffs. Simultaneously these results highlight the critical importance of including battery degradation considerations in the operational planning of the ESS.

E. DISCUSSION

In microgrid operations, cost savings realized by accounting for ESS battery degradation are achieved by strategically managing the SoC and DoD at their optimal low levels, taking into account both electricity rates and depreciation. While the conventional approach involves charging the ESS during periods of low electricity rates, it is vital to delay the charging time to optimize the SoC. In addition, we highlight that during significant battery degradation phases, particularly at high SoH levels, the model inherently optimizes for a conservative battery operation strategy. This optimization occurs not through artificially imposed SoC constraints, but by allowing the model to determine the optimal charge-discharge actions based on degradation considerations. This approach naturally results in operations that favor a lower SoC range, thereby minimizing DoD without the need for predefined SoC limits.

When incorporating battery degradation into the operation of the ESS, there may be instances where charge-discharge scenarios seem less efficient compared to when only considering electricity rates. This is due to the reduction in ESS degradation offsetting losses from electricity costs. Since implementing this approach mandates a sophisticated battery degradation model and a comprehensive objective function within a framework, this study thus introduces a viable candidate for utilizing QP.

V. CONCLUSION

Microgrids play a vital role in modern power systems, offering improved resilience, sustainability, and energy efficiency. As these systems incorporate elements such as PV, ESS, and ToU tariffs, optimizing their operations becomes crucial. Given the high costs and inevitable wear of batteries over time, it is important to account for their degradation when determining the most cost-effective operation strategies.

This research addresses the shortcomings of past microgrid optimization methods, which often overlooked or inadequately tackled battery degradation. We have introduced an advanced quadratic battery degradation model that captures both SoC and DoD dynamics. Incorporating the financial impacts of degradation into our optimization process made our approach both practical and financially insightful.

Applying QP to our refined problem, we observed a notable reduction in operational costs ranging from 3% to 18%. This optimization not only streamlines operations but also demonstrates a keen understanding of the financial implications of battery wear.

The findings of this study contribute to advancing smarter microgrid operations. By incorporating precise insights into battery degradation in the optimization process, decision-makers can achieve a balance between efficient operations and battery lifespan.

In this study, we focused on the integration of PV and ESS systems in an educational institution setting. However, we believe that our research has the potential to extend to various industrial applications beyond microgrid operation. For example, our proposed degradation model could be applied to Electric Vehicles (EVs) to develop optimal charging strategies that mitigate battery degradation. By considering the specific characteristics of EV batteries and their usage patterns, our model could help extend the lifespan of EV batteries and reduce the overall cost of ownership for EV users.

Furthermore, our study could be extended to optimize the installation capacity and the number of energy storage systems. Future studies may leverage our QP formulation to analyze the economic benefits of different battery configurations and identify the optimal capacity for specific applications. Additionally, investigating the potential economic advantages of using multiple batteries with lower individual SoH could be a valuable area for further research. These extensions could help maximize the industrial value of ESSs by leveraging analytical optimizations and the quadratic degradation model.

APPENDIX
QP FORMULATION DERIVATION

To represent the objective function in matrix form, we define the following vectors:[1]

$$\mathbf{P}^{GRID} = \begin{pmatrix} P_0^{GRID} \\ P_1^{GRID} \\ \vdots \\ P_{N-1}^{GRID} \end{pmatrix}, \ \mathbf{P}^{ESS} = \begin{pmatrix} P_0^{ESS} \\ P_1^{ESS} \\ \vdots \\ P_{N-1}^{ESS} \end{pmatrix},$$

$$\mathbf{B}^{SoC} = \begin{pmatrix} B_0^{SoC} \\ B_1^{SoC} \\ \vdots \\ B_{N-1}^{SoC} \end{pmatrix}, \ \mathbf{B}^{SoC'} = \begin{pmatrix} B_1^{SoC} \\ B_2^{SoC} \\ \vdots \\ B_N^{SoC} \end{pmatrix}.$$

The relationship (9) can be represented in matrix form as follows:

$$\mathbf{P}^{GRID} = \mathbf{P}^{ESS} + \mathbf{P}^{LOAD} - \mathbf{P}^{PV}. \tag{15}$$

The vector $\mathbf{B}^{SoC}$ and its lead vector $\mathbf{B}^{SoC'}$ can be represented as follows:

$$\mathbf{B}^{SoC} = B_0^{SoC}\mathbb{1}_N + \mathbf{M}\mathbf{P}^{ESS}/q^{ESS}, \tag{16}$$

$$\mathbf{B}^{SoC'} = B_0^{SoC}\mathbb{1}_N + \mathbf{M}'\mathbf{P}^{ESS}/q^{ESS}, \tag{17}$$

where

$$\mathbf{M} = \begin{pmatrix} 0 & 0 & \dots & 0 & 0 \\ 1 & 0 & \dots & 0 & 0 \\ 1 & 1 & \dots & 0 & 0 \\ & & \vdots & & \\ 1 & 1 & \dots & 1 & 0 \end{pmatrix}, \quad \mathbf{M}' = \begin{pmatrix} 1 & 0 & \dots & 0 & 0 \\ 1 & 1 & \dots & 0 & 0 \\ 1 & 1 & \dots & 0 & 0 \\ & & \vdots & & \\ 1 & 1 & \dots & 1 & 1 \end{pmatrix}.$$

Applying the above to the objective function yields the following:

$$\begin{aligned} J = \min_{\mathbf{P}^{ESS}} & \mathbf{C}^{GRID} \cdot (\mathbf{P}^{ESS} + \mathbf{P}^{LOAD} - \mathbf{P}^{PV}) \\ & + c^{new}[\beta_0 N + \beta_1(2NB_0^{SoC} + \frac{1}{q^{ESS}}\mathbb{1}_N^T(\mathbf{M}+\mathbf{M}')\mathbf{P}^{ESS}) \\ & + \beta_2(\frac{1}{q^{ESS}})^2\mathbf{P}^{ESS}\cdot\mathbf{P}^{ESS}]. \end{aligned} \tag{18}$$

Excluding the constant term,

$$\begin{aligned} J = \min_{\mathbf{P}^{ESS}} & \mathbf{C}^{GRID} \cdot \mathbf{P}^{ESS} + \frac{c^{new}\beta_1}{q^{ESS}}\mathbb{1}_N^T(\mathbf{M}+\mathbf{M}')\mathbf{P}^{ESS} \\ & + \frac{c^{new}\beta_2}{(q^{ESS})^2}\mathbf{P}^{ESS}\cdot\mathbf{P}^{ESS}. \end{aligned} \tag{19}$$

It can be rearranged into the general form of a QP problem as follows:

$$J = \min_{\mathbf{P}^{ESS}} \frac{1}{2}(\mathbf{P}^{ESS})^T\mathbf{Q}\mathbf{P}^{ESS} + \mathbf{b}\cdot\mathbf{P}^{ESS}, \tag{20}$$

[1] $\mathbf{C}^{GRID}$, $\mathbf{P}^{PV}$, $\mathbf{P}^{LOAD}$ are also defined in the same manner.

where

$$\mathbf{Q} = \frac{2c^{new}\beta_2}{(q^{ESS})^2}\mathbf{I_N}, \tag{21}$$

$$\mathbf{b} = \mathbf{C}^{GRID} + \frac{c^{new}\beta_1}{q^{ESS}}(\mathbf{M}+\mathbf{M}')^T\mathbb{1}_N. \tag{22}$$

The second inequality of the constraint condition (6) can be rewritten as follows, according to the relation equation (9):

$$P_t^{ESS} \le P_{max}^{GRID} - P_t^{LOAD} + P_t^{PV}. \tag{23}$$

Therefore, this can be combined with constraint condition (7):

$$P_t^{ESS} \le min\{P_{max}^{GRID} - P_t^{LOAD} + P_t^{PV}, P_{max}^{ESS}\}. \tag{24}$$

Accordingly, we define the upper and lower boundary matrices and express the constraint condition in the form of the P_{ESS} matrix:

$$\mathbf{P}^{LB} \le \mathbf{P}^{ESS} \le \mathbf{P}^{UB}, \tag{25}$$

where

$$P_i^{LB} = min\{P_{min}^{GRID} - P_i^{LOAD} + P_i^{PV}, P_{min}^{ESS}\},$$
$$P_i^{UB} = min\{P_{max}^{GRID} - P_i^{LOAD} + P_i^{PV}, P_{max}^{ESS}\}.$$

To summarize the above, constraint conditions (6), (7), and (8) are arranged in the following matrix form:

$$\begin{pmatrix} \mathbf{I}_N \\ -\mathbf{I}_N \\ \mathbf{M} \\ -\mathbf{M} \end{pmatrix} P_{ESS} \le \begin{pmatrix} \mathbf{P}^{UB} \\ -\mathbf{P}^{LB} \\ q^{ESS}(B_{max}^{SoC} - B_0^{SoC})\mathbb{1}_N \\ q^{ESS}(-B_{min}^{SoC} + B_0^{SoC})\mathbb{1}_N \end{pmatrix}.$$

REFERENCES

[1] A. Hirsch, Y. Parag, and J. Guerrero, "Microgrids: A review of technologies, key drivers, and outstanding issues," *Renew. Sustain. Energy Rev.*, vol. 90, pp. 402–411, Jul. 2018.
[2] S. P. Bihari, P. K. Sadhu, K. Sarita, B. Khan, L. D. Arya, R. K. Saket, and D. P. Kothari, "A comprehensive review of microgrid control mechanism and impact assessment for hybrid renewable energy integration," *IEEE Access*, vol. 9, pp. 88942–88958, 2021.
[3] A. Parisio, E. Rikos, and L. Glielmo, "A model predictive control approach to microgrid operation optimization," *IEEE Trans. Control Syst. Technol.*, vol. 22, no. 5, pp. 1813–1827, Sep. 2014.
[4] A. Nawaz, J. Wu, J. Ye, Y. Dong, and C. Long, "Distributed MPC-based energy scheduling for islanded multi-microgrid considering battery degradation and cyclic life deterioration," *Appl. Energy*, vol. 329, Jan. 2023, Art. no. 120168.
[5] I. Shafikhani, C. Sundström, J. Åslund, and E. Frisk, "MPC-based energy management system design for a series HEV with battery life optimization," in *Proc. Eur. Control Conf. (ECC)*, Jun. 2021, pp. 2591–2596.
[6] C. Ju, P. Wang, L. Goel, and Y. Xu, "A two-layer energy management system for microgrids with hybrid energy storage considering degradation costs," *IEEE Trans. Smart Grid*, vol. 9, no. 6, pp. 6047–6057, Nov. 2018.
[7] W. Li, N. Wang, A. Garg, and L. Gao, "Multi-objective optimization of an air cooling battery thermal management system considering battery degradation and parasitic power loss," *J. Energy Storage*, vol. 58, Feb. 2023, Art. no. 106382.
[8] Y. Wu, Z. Liu, J. Liu, H. Xiao, R. Liu, and L. Zhang, "Optimal battery capacity of grid-connected PV-battery systems considering battery degradation," *Renew. Energy*, vol. 181, pp. 10–23, Jan. 2022.

[9] K. Ginigeme and Z. Wang, "Distributed optimal vehicle-to-grid approaches with consideration of battery degradation cost under real-time pricing," *IEEE Access*, vol. 8, pp. 5225–5235, 2020.
[10] J. Cao, D. Harrold, Z. Fan, T. Morstyn, D. Healey, and K. Li, "Deep reinforcement learning-based energy storage arbitrage with accurate lithium-ion battery degradation model," *IEEE Trans. Smart Grid*, vol. 11, no. 5, pp. 4513–4521, Sep. 2020.
[11] B. Xu, A. Oudalov, A. Ulbig, G. Andersson, and D. S. Kirschen, "Modeling of lithium-ion battery degradation for cell life assessment," *IEEE Trans. Smart Grid*, vol. 9, no. 2, pp. 1131–1140, Mar. 2018.
[12] M. Safari, M. Morcrette, A. Teyssot, and C. Delacourt, "Multimodal physics-based aging model for life prediction of Li-ion batteries," *J. Electrochemical Soc.*, vol. 156, no. 3, p. A145, 2009.
[13] Q. Zhang and R. E. White, "Capacity fade analysis of a lithium ion cell," *J. Power Sources*, vol. 179, no. 2, pp. 793–798, May 2008.
[14] J. Vetter, P. Novák, M. R. Wagner, C. Veit, K.-C. Möller, J. Besenhard, M. Winter, M. Wohlfahrt-Mehrens, C. Vogler, and A. Hammouche, "Ageing mechanisms in lithium-ion batteries," *J. Power Sources*, vol. 147, nos. 1–2, pp. 269–281, Sep. 2005.
[15] I. Laresgoiti, S. Käbitz, M. Ecker, and D. U. Sauer, "Modeling mechanical degradation in lithium ion batteries during cycling: Solid electrolyte interphase fracture," *J. Power Sources*, vol. 300, pp. 112–122, Dec. 2015.
[16] J. Park, T. Kwon, and M. K. Sim, "Optimal energy storage system control using a Markovian degradation model—Reinforcement learning approach," *J. Energy Storage*, vol. 71, Nov. 2023, Art. no. 107964.
[17] G. G. Yen and T. W. Hickey, "Reinforcement learning algorithms for robotic navigation in dynamic environments," *ISA Trans.*, vol. 43, no. 2, pp. 217–230, Apr. 2004.
[18] O. D. Montoya, W. Gil-González, and A. Garces, "Sequential quadratic programming models for solving the OPF problem in DC grids," *Electr. Power Syst. Res.*, vol. 169, pp. 18–23, Apr. 2019.
[19] D. M. Teferra, L. M. H. Ngoo, and G. N. Nyakoe, "Fuzzy-based prediction of solar PV and wind power generation for microgrid modeling using particle swarm optimization," *Heliyon*, vol. 9, no. 1, Jan. 2023, Art. no. e12802.
[20] M. Esmaeili, A. A. Ahmadi, A. Nateghi, and M. Shafie-khah, "Robust power management system with generation and demand prediction and critical loads in DC microgrid," *J. Cleaner Prod.*, vol. 384, Jan. 2023, Art. no. 135490.
[21] S. Kallio and M. Siroux, "Photovoltaic power prediction for solar microgrid optimal control," *Energy Rep.*, vol. 9, pp. 594–601, Mar. 2023.
[22] S. Wu, T. Liu, M. Egerstedt, and Z.-P. Jiang, "Quadratic programming for continuous control of safety-critical multi-agent systems under uncertainty," *IEEE Trans. Autom. Control*, vol. 68, no. 11, pp. 6664–6679, 2023.
[23] C. Yoon, Y. Park, M. K. Sim, and Y. I. Lee, "A quadratic programming-based power dispatch method for a DC-microgrid," *IEEE Access*, vol. 8, pp. 211924–211936, 2020.
[24] M. Sharafi and T. Y. ELMekkawy, "Multi-objective optimal design of hybrid renewable energy systems using PSO-simulation based approach," *Renew. Energy*, vol. 68, pp. 67–79, Aug. 2014.
[25] L. O. P. Vásquez, J. L. Redondo, J. D. Á. Hervás, V. M. Ramírez, and J. L. Torres, "Balancing CO_2 emissions and economic cost in a microgrid through an energy management system using MPC and multi-objective optimization," *Appl. Energy*, vol. 347, Oct. 2023, Art. no. 120998.
[26] F. A. Mohamed and H. N. Koivo, "Multiobjective optimization using mesh adaptive direct search for power dispatch problem of microgrid," *Int. J. Electr. Power Energy Syst.*, vol. 42, no. 1, pp. 728–735, Nov. 2012.
[27] M. Borghei and M. Ghassemi, "A multi-objective optimization scheme for resilient, cost-effective planning of microgrids," *IEEE Access*, vol. 8, pp. 206325–206341, 2020.
[28] A. Su and G. Yerui, "Multi objective optimal dispatching of microgrid considering multiple random variables based on improved NSGA-III," in *Proc. IEEE 4th Int. Electr. Energy Conf. (CIEEC)*, May 2021, pp. 1–6.
[29] Y. Huang, H. Masrur, M. S. H. Lipu, H. O. R. Howlader, M. M. Gamil, A. Nakadomari, P. Mandal, and T. Senjyu, "Multi-objective optimization of campus microgrid system considering electric vehicle charging load integrated to power grid," *Sustain. Cities Soc.*, vol. 98, Nov. 2023, Art. no. 104778.
[30] X. Han, L. Lu, Y. Zheng, X. Feng, Z. Li, J. Li, and M. Ouyang, "A review on the key issues of the lithium ion battery degradation among the whole life cycle," *eTransportation*, vol. 1, Aug. 2019, Art. no. 100005.
[31] S. Downing and D. Socie, "Simple rainflow counting algorithms," *Int. J. Fatigue*, vol. 4, no. 1, pp. 31–40, Jan. 1982.
[32] A. Mamun, I. Narayanan, D. Wang, A. Sivasubramaniam, and H. K. Fathy, "Multi-objective optimization of demand response in a datacenter with lithium-ion battery storage," *J. Energy Storage*, vol. 7, pp. 258–269, Aug. 2016.
[33] J. Lacap, J. W. Park, and L. Beslow, "Development and demonstration of microgrid system utilizing second-life electric vehicle batteries," *J. Energy Storage*, vol. 41, Sep. 2021, Art. no. 102837.
[34] K. Ziat, H. Louahlia, I. Voicu, and P. Schaetzel, "Impact of the battery SOC range on the battery heat generation and maximum temperature rise," *J. Thermal Anal. Calorimetry*, vol. 148, no. 20, pp. 10857–10870, Oct. 2023.

KYONG JIN CHOI received the B.S. degree in physics from Seoul National University, Seoul, South Korea, in 2002, and the M.S. degree in investment business administration and the Ph.D. degree in finance from Korea University, Seoul, in 2008 and 2018, respectively. Currently, he is a Research Professor with the Energy and Environment Research Institute, Seoul National University of Science and Technology (SeoulTech), Seoul. His research interests include deep reinforcement learning-based optimal control, smart grids, and financial market anomalies.

JAEMIN PARK received the dual B.S. degree in industrial engineering and information technology and management from Seoul National University of Science and Technology (SeoulTech), Seoul, South Korea, and Northumbria University, New Castle, U.K., in 2023. He is currently pursuing the M.S. degree in data science with SeoulTech. Since 2020, he has been a Student Researcher with the Laboratory of Applied Probability, SeoulTech. His research interests include deep reinforcement learning with applications in energy systems and smart grid.

TAEHYEON KWON (Member, IEEE) received the dual B.S. degree in information technology and management from Seoul National University of Science and Technology (SeoulTech) and Northumbria University, in 2023. He is currently pursuing the Ph.D. degree in industrial and manufacturing engineering with The Pennsylvania State University, State College, PA, USA.

He was a Researcher with the Energy and Environment Research Institute, SeoulTech, from February 2023 to August 2023. His main research interest includes multi-horizon stochastic optimization with deep neural networks.

SOONHYUNG KWON received the B.S. degree in electrical and information engineering from Seoul National University of Science and Technology (SeoulTech), Seoul, South Korea, in 2021, where he is currently pursuing the M.S. degree. His research interests include power electronics and smart grid.

DO-HOON KWON (Member, IEEE) received the B.S., M.S., and Ph.D. degrees in electrical engineering from Seoul National University, Seoul, South Korea, in 2010, 2012, and 2018, respectively.

From 2018 to 2021, he was with Korea Electrotechnology Research Institute, as a Senior Researcher. He is currently an Assistant Professor with the Department of Electrical and Information Engineering, Seoul National University of Science and Technology, Seoul. His research interests include HVDC systems, renewable energy integration in power systems, and smart power networks. He was a recipient of the Best Reviewer Award for IEEE TRANSACTIONS ON SMART GRID, in 2017.

YOUNG-IL LEE (Senior Member, IEEE) received the B.S., M.S., and Ph.D. degrees in control and instrumentation engineering from Seoul National University (SNU), in 1986, 1988, and 1994, respectively. He was with Gyeongsang National University, from 1994 to 2001, and moved to Seoul National university of Science and Technology (SeoulTech), in 2001. He was a Visiting Research Fellow with the Department of Engineering Science, Oxford University, from 1998 to 1999 and 2007. He is currently a Professor with the Department of Electrical and Information Engineering, SeoulTech. He is the Director of the Research Center of Electrical and Information Technology, SeoulTech. His research interests include MPC for systems with input constraints and model uncertainties, MPC method for various converters and inverters, control of EV chargers, control of AC motors for EV application, and energy management algorithm of micro-grids. He is serving as an Editor for *International Journal of Control, Automation, and Systems* (IJCAS) and *International Journal of Automotive Technology* (IJAT), in 2017 and 2019, respectively.

MIN KYU SIM (Member, IEEE) received the Ph.D. degree in industrial engineering from Georgia Institute of Technology, Atlanta, GA, USA, in 2014. From 2015 to 2017, he was a Portfolio Manager and a Quantitative Researcher of asset management firms. From 2018 to 2019, he was a Research Professor with the Smart Energy Research Center, Kyung Hee University, South Korea. Since September 2019, he has been an Assistant/Associate Professor with the Department of Data Science and the Department of Industrial Engineering, Seoul National University of Science and Technology (SeoulTech), Seoul, South Korea. His research interests include stochastic processes application, reinforcement learning-based optimal control, and quantitative finance.